Journal of the Indian Society of Soil Science, Vol. 66, No. 1, pp 20-27 (2018)
DOI: 10.5958/0974-0228.2018.00003.8

Geostatistical and Multivariate Analysis of Heavy Metal Pollution of Coal-mine Affected Agricultural Soils of North-eastern India

S.K. Reza*, S.K. Ray[1], D.C. Nayak and S.K. Singh[2]
ICAR-National Bureau of Soil Survey and Land Use Planning,
Sector-II, DK-Block, Salt Lake, Kolkata, West Bengal

Total concentrations of heavy metals in the soils of mine drainage and surrounding agricultural fields in the Ledo coal mining area of Tinsukia district, Assam, India, were investigated using statistics, geostatistics and GIS techniques. The amounts of iron (Fe), manganese (Mn) and zinc (Zn) were determined from 83 soil samples collected within the contaminated area. The mean concentration of Fe, Mn and Zn were 28585, 627 and 227 mg kg^{-1}, respectively. The greatest and the smallest standard deviation were observed in the Fe (7506) and pH (0.44), respectively. All heavy metals exhibited a medium variation (15-50%). Analysis of the isotropic variogram indicated that the Mn and Zn semivariograms were well-described with the exponential model, with the distance of spatial dependence being 1083 and 994 m, respectively, while the Fe semivariogram was well-described with the spherical model, with the distance of spatial dependence being 1784 m. Thus, the length of the spatial autocorrelation was much longer than the sampling interval of 500 m. The spatial distribution maps of Fe, Mn and Zn showed that high concentration of heavy metals was located in the low-lying rice field and near coal mining site. Multivariate statistical analyses and principal component analysis suggested that Fe was derived from anthropogenic sources, particularly coal mining activities, whereas Mn and Zn were derived from lithogenic and/or anthropogenic sources.

Key words: Coal-mine, heavy metals, geostatistics, principal component, multivariate analysis

Coal plays an important role in energy generation, and ~27% of the world's energy consumption originates from the incineration of coal (Bhuiyan *et al.* 2010). Underground and open pit coal exploitation includes a phase development in mine and removal of surrounding rocks, which are low in coal content (<30%) and often contain iron sulphide minerals. During the process of opencast and underground coal mining, a variety of rock types with different compositions are exposed to atmospheric conditions and undergo accelerated weathering (Reza *et al.* 2015). These waste materials typically contain variable amounts of sulphide minerals. After disposal, exposure to atmospheric oxygen and water results in sulphide oxidation and the formation of acid mine drainage (AMD) with variable pH, SO_4^{2-}, and heavy metal content (Silva *et al.* 2011).

When coal is mined, pyrite (FeS_2) is exposed to oxygen and water, setting off a series of reactions that can result in lowered pH (unless there are sufficient carbonates to neutralize acids produced by oxidation and hydrolysis) and the release of high concentrations of metals, such as iron (Fe), aluminum (Al), and manganese (Mn) (Adriano 2001). In addition to causing poor water quality, mine drainage can affect the substrate of a stream. Ferrous iron (Fe^{2+}) is oxidized to ferric iron (Fe^{3+}) to form a precipitate on the substrate (commonly referred to as ''yellow boy'') in the presence of water when the pH is greater than about 3.5 (Rose and Cravotta 1998). In many mine drainage streams with a relatively high pH, precipitated Fe and Al may coat the stream substrate and cause an unstable habitat for macro-invertebrates (Simmons *et al.* 2005).

Earlier studies on environmental impacts of coal mining have shown that soil acidity, toxic metal concentrations (Adriano 2001) and vegetation damage (Madejón *et al.* 2002) are the predominant negative impacts of AMD. Seepage of water from overburden

*Corresponding author (Email: reza_ssac@yahoo.co.in)
Present address
[1]ICAR-National Bureau of Soil Survey and Land Use Planning, Jamuguri Road, Jorhat, Assam
[2]ICAR-National Bureau of Soil Survey and Land Use Planning, Nagpur, Maharashtra

dumps, exposed overburden and coal processing *etc.* constitutes mining effluent, which contains heavy metals (Wong 2003). Pollution of the natural environment by heavy metals is a worldwide problem because these metals are indestructible and most of them have toxic effects on living organisms at certain concentrations (MacFarlane and Burchett 2002).

Geostatistics originated from the mining and petroleum industries began with the work by Danie G. Krige in the 1950s, and it was further developed by Georges Matheron in the 1960s. Today, geostatistics has been extended to many other fields related to the earth sciences. Geostatistics is a technology for estimating the soil property values in non-sampled areas or areas with sparse samplings (Yao *et al.* 2004). These non-sampled areas can vary in space (in one, two or three dimensions) from the sampled data (Zhu *et al.* 2005). Geostatistics provides a set of statistical tools for a description of spatial patterns, quantitative modeling of spatial continuity, spatial prediction, and uncertainty assessment (Goovaerts 1999). Geostatistical techniques incorporating spatial information into predictions can improve estimation and enhance map quality (Mueller and Pierce 2003). Several geostatistical methods have been used by the researchers for developing the spatial distribution maps of heavy metal in soil, depending upon the requirements and situations of field experiments. Among different methods of spatial interpolation, ordinary kriging is most common (Franzen and Peck 1993). Kriging is a useful tool to predict and interpolate data between measured locations (Reza *et al.* 2010, 2012, 2014, 2016a, 2016b, 2016c, 2017).

In the north-eastern India, coalfields are confined particularly in the Tinsukia district of upper Assam. Coal mining activities in these areas have been in operation since 1882. Most of the coalfields now been closed due to declining of production while the collieries of Tikka, Borgolai, Ledo, Tipang and Namdang of Makum coalfield have so far produced more than 25 million tonnes (Mt) of coal out of the reserve estimated at 130 Mt up to a depth of 300 m (Nesa and Azad 2008). These fields are still under operation in full swing. Our study investigates the extent of contamination of heavy metals (Fe, Mn and Zn) in soil by Ledo coal mine using geostatistics and GIS techniques to reveal the spatial distribution patterns and provides a basis for hazard assessment.

Material and Methods

Study area

The study was carried out near the Ledo coal mining area of Tinsukia district, Assam, north-eastern India, extended between 27°17′05″ to 27°20′45″ N latitude and 95°39′35″ to 95°44′53″ E longitude covering an area of 20 km^2 (Fig. 1). The climate is

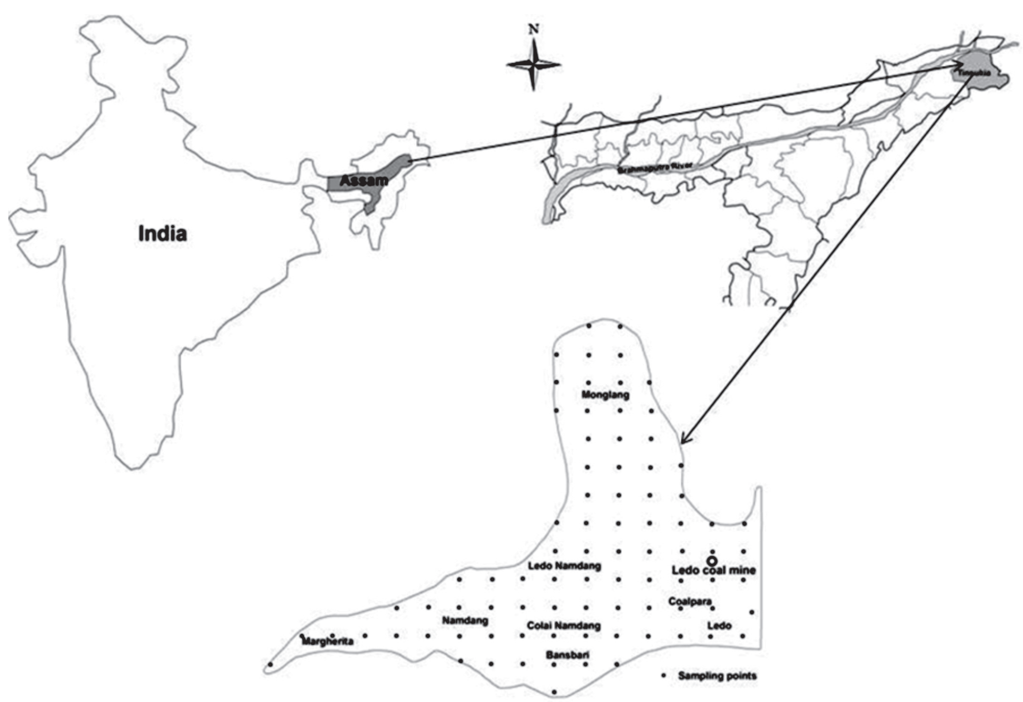

Fig. 1. Location and grid map of the study area

humid subtropical. The average annual rainfall ranges between 2000-2500 mm with maximum rainfall during July-September. The climate is moderately warm during summer but cold in winter. Mean monthly minimum and maximum temperatures were 7 and 36 °C, respectively.

Soil sampling and analysis

Eighty three surface soil samples were collected from a depth of 0-25 cm (plough layer) using a square 500 m×500 m grid (Fig. 1), corresponding to a sampling density of 4 samples per km^2 covering not only the waste disposal site, but also the surrounding cultivated areas with the help of a hand-held global positioning system. Soil samples were air-dried and ground to pass through a 2-mm sieve. A combined glass calomel electrode was used to determine the pH of aqueous suspension (1:2.5 soil:solution ratio). Organic carbon (OC) was determined by the Walkley and Black (1934) method. Digestion of 0.50 g soil samples was performed with concentrated HNO_3, HF and $HClO_4$ in a microwave digester (Model Start D, Milestone). Subsequently, the total concentration of heavy metals was determined by a Shimadzu AA6300 atomic absorption spectrophotometer.

Geostatistical analysis based on GIS

Spatial interpolation and GIS mapping techniques were employed to produce spatial distribution and risk assessment maps for the three investigated heavy metals, and the software used for this purpose was ArcGIS v.9.3.1 (ESRI Co, Redlands, USA). In ArcGIS, kriging can express the spatial variation and allow a variety of map outputs, and at the same time minimize the errors of predicted values. Moreover, it is very flexible and allows users to investigate graphs of spatial autocorrelation. Kriging, as applied within moving data neighborhoods, is a non-stationary algorithm which corresponds to a non-stationary random function model with varying mean but stationary covariance (Deutsch and Journal 1992). In kriging, a semivariogram model was used to define the weights of the function (Webster and Oliver 2001), and the semivariance is an autocorrelation statistic defined as follows (Mabit and Bernard 2007):

$$\gamma(h) = \frac{1}{2N(h)} \sum_{i=1}^{N(h)} [z(x_i) - z(x_i + h)]^2 \quad \ldots(1)$$

where, $z(x_i)$ is the value of the variable z at location of x_i, h the lag and $N(h)$ the number of pairs of sample points separated by h. For irregular sampling, it is rare for the distance between the sample pairs to be exactly equal to h. That is, h is often represented by a distance band.

Ordinary kriging (OK) is known to be an estimator in the sense that observation points are re-estimated with the minimum error. This method does not necessarily require observation networks where data are normally distributed, and for the estimation of the spatial correlation of the regionalized variables, only the neighboring points of estimation data are taken into consideration (De Marsily 1986).

Anisotropic semivariograms did not show any differences in spatial dependence based on direction, for which reason isotropic semivariograms were chosen. Circular, spherical, exponential and Gaussian models were fitted to the empirical semivariograms. Best-fit model with minimum root mean square error (RMSE) (Eq. 2) were selected for each heavy metal:

$$\mathrm{RMSE} = \sqrt{\frac{1}{N} \sum_{i=1}^{N} \left[z(x_i) - \hat{z}(x_i)\right]^2} \quad \ldots(2)$$

Using the model semivariogram, basic spatial parameters such as nugget (C_0), sill ($C + C_0$) and range (A) was calculated which provide information about the structure as well as the input parameters for the kriging interpolation. Nugget is the variance at zero distance, sill is the lag distance between measurements at which one value for a variable does not influence neighboring values and range is the distance at which values of one variable become spatially independent of another (Lopez-Granadoz *et al.* 2002). Geostatistical analysis consisting of semivariogram calculation, cross-validation and mapping was performed using the geostatistical analyst extension of ArcGIS v.9.3.1 (ESRI Co, Redlands, USA).

Accuracy of the maps was evaluated through cross-validation approach (Davis 1987; Reza *et al.* 2010). Among three evaluation indices used in this study, mean absolute error (MAE), and mean squared error (MSE) measure the accuracy of prediction, whereas goodness of prediction (G) measures the effectiveness of prediction. The MAE is a measure of the sum of the residuals (Voltz and Webster 1990).

$$\mathrm{MAE} = \frac{1}{N} \sum_{i=1}^{N} \left[z(x_i) - \hat{z}(x_i)\right] \quad \ldots(3)$$

where, $\hat{z}(x_i)$ is the predicted value at location i. Small MAE values indicate less error. The MAE measure, however, does not reveal the magnitude of error that might occur at any point and hence MSE will be calculated as:

$$MSE = \frac{1}{N}\sum_{i=1}^{N}\left[z(x_i) - \hat{z}(x_i)\right] \quad ...(4)$$

Squaring the difference at any point gives an indication of the magnitude, *e.g.* small MSE values indicate more accurate estimation, point-by-point. The *G* measure gives an indication of how effective a prediction might be relative to that which could have been derived from using the sample mean alone (Schloeder *et al.* 2001).

$$G = \left[1 - \frac{\sum_{i=1}^{N}\left[z(x_i) - \hat{z}(x_i)\right]^2}{\sum_{i=1}^{N}\left[z(x_i) - \bar{z}\right]^2}\right] \times 100 \quad ...(5)$$

where, z is the sample mean. If G = 100, it indicates perfect prediction, while negative values indicate that the predictions are less reliable than using sample mean as the predictors. The comparison of performance between interpolations was achieved by MAE.

Multivariate statistical analysis

The identification of pollutants sources is conducted with the aid of multivariate statistical analyses, such as principal component analysis (PCA) and correlation analysis. Multivariate analyses of the data in this work were carried out by SPSS v.16.0 software (SPSS Inc., Chicago, USA). Bartlett sphericity test and Kaiser-Mayer-Olkin test indicated that the normalized data were suitable for PCA. Varimax with Kaiser Normalization rotation was applied to maximize the variances of the factor loadings across variances for each factor.

Results and Discussion

Descriptive statistics of heavy metals and other soil properties

The statistical characteristics of soil Fe, Mn and Zn are listed in table 1. In the present investigation, the pH ranged from 3.7 to 5.7 with the mean values 4.7. The values of OC ranged from 0.13 to 6.76% with mean value of 1.59%. The mean concentration of Fe, Mn and Zn were 28585, 627.1 and 226.9 mg kg^{-1}, respectively. A high mean concentration of Fe (59853 mg kg^{-1}) and Mn (1886 mg kg^{-1}) has also been reported in coal-mine affected agricultural soils (Bhuiyan *et al.* 2010). The release of high metal content in the mine drainage soil is dependent on the weathering effects of mine drainage water (Banwart and Malmstrom 2001). Pyrite weathering releases soluble ferrous iron (Fe^{2+}) and acidity that is represented by production of protons (Eq. 6):

$$FeS_2(s) + H_2O + 3\tfrac{1}{2}O_2(aq) \rightarrow Fe^{2+} + 2SO_4^{2-} + 2H^+ \quad ...(6)$$

If sufficient dissolved oxygen is present or solutions is oxygenated by contact with the atmosphere, the dissolved Fe^{2+} would be oxidized to Fe^{3+}, consuming acidity in the process (Eq. 7):

$$2Fe^{2+} + \tfrac{1}{2}O_2 + 2H^+ \rightarrow 2Fe^{3+} + H_2O \quad ...(7)$$

When Fe^{3+} reacts further to precipitate as iron oxyhydroxide minerals, a much greater net production of acidity occurs (Eq. 8):

$$Fe^{3+} + 3H_2O \leftrightarrow Fe(OH)_3(s) + 3H^+ \quad ...(8)$$

This may react with pyrite to produce more acidity and ferrous iron (Eq. 9):

$$14Fe^{3+} + FeS_2(s) + 8H_2O \rightarrow 2SO_4^{2-} + 15Fe^{2+} + 16H^+ \quad ...(9)$$

The Fe^{2+} produced by the earlier reaction is re-oxidized by available dissolved oxygen, perpetuating the cycle represented by the reactions (Eqs. 6-9). Similarly, Mn is released from siderite (Sakurovs *et al.* 2007).

Metal sulphides other than pyrite will not necessarily produce acidity, but will release soluble metal ions to solution. For example, sphalerite (ZnS) will release Zn into the environment by oxidization through the reaction below (Eq. 10):

$$ZnS(s) + 2O_2(aq) \rightarrow Zn^{2+} + SO_4^{2-} \quad ...(10)$$

Table 1. Summary statistics of heavy metal concentrations and selected soil properties

Statistics	pH	Organic carbon (%)	Fe	Mn (mg kg^{-1})	Zn
Mean	4.7	1.59	28585	627.1	226.9
SD*	0.44	0.96	7506	252.5	84.9
CV (%)**	9.4	60.4	26.3	40.3	37.5
Minimum	3.7	0.13	12448	129.2	18.9
Maximum	5.7	6.76	41938	1226.8	450.0
Skewness	0.10	2.30	-0.22	0.13	0.23
Kurtosis	-0.39	9.22	-0.94	-0.53	-0.10
Distribution pattern			Normal	Normal	Normal

*Standard Deviation; **Coefficient of Variation

The greatest and the smallest standard deviation were observed in the Fe (7506) and pH (0.44), respectively. Similar observations also documented a higher standard deviation of Fe as compared to other heavy metals in polluted agricultural soils (Reza *et al.* 2016d). All the heavy metals exhibit a medium variation (15-50%) according to guidelines provided by Warrick (1998). Skewness is the most common form of departure from normality. If a variable has positive skewness, the confidence limits on the variogram are wider than they would otherwise be and consequently, the variances are less reliable. Besides, normality may not be strictly required in geostatistical analyses but normal distribution may lead to more reliable results (Webster and Oliver 2001). Therefore, the data distribution was tested for normality using the Kolmogorov-Smirnov test. All the studied heavy metals were normally distributed (Table 1).

Semivariogram analysis of heavy metals

Semivariogram parameters (nugget, sill and range) for each heavy metal with best-fitted model was identified based on minimum root mean square error (RMSE). Analysis of the isotropic variogram indicated that the Mn and Zn semivariograms were well described with the exponential model, with the distance of spatial dependence being 1083 and 994 m, respectively, while the Fe semivariogram was well described with the spherical model, with the distance of spatial dependence being 1784 m (Table 2) thus, the length of the spatial autocorrelation was much longer than the sampling interval of 500 m. Therefore, the current sampling design is appropriate for this study and it is expected that a good spatial structure would be shown on the interpolated map.

The ratio of nugget and sill is commonly used to express the spatial autocorrelation of regional variables, which also indicates the predominant factors among all natural and anthropogenic factors (Robertson *et al.* 1997). The ratios of nugget and sill between 0.25 and 0.75 represented moderate spatial dependence; those below 0.25 represented strong spatial dependence; and all others represented weak dependence. All the studied heavy metals were moderately spatially dependent suggesting that they are affected by either anthropogenic or natural factors or both.

Spatial distribution of heavy metals pollution

Using the available measurements for Fe, Mn and Zn concentration as well as the aforementioned structural models, spatial distribution maps of these heavy metals were produced using the ordinary kriging procedure (Journel and Huijbregts 1978). The spatial distribution maps of Fe, Mn and Zn (Fig. 2) showed that high concentration of heavy metals was located in the low-lying rice field and near coal mining site. Evaluation indices resulting from cross-validation of spatial distribution maps (Table 3) for all the soil heavy metals the prediction of goodness (*G*) value was greater than zero, which indicates that spatial prediction using semivariogram parameters is better than assuming mean of observed value as the values for any unsampled location. This also shows that semivariogram parameters obtained from fitting of experimental semivariogram values were fairly reasonable to describe the spatial variation.

Source identification based on multivariate statistics

For further evaluation of extent of metal contamination in the study area and source identification, PCA was used following standard procedure reported in literature (Bhuiyan *et al.* 2010; Reza *et al.* 2013, 2015). Varimax rotation (Franco-Uría *et al.* 2009) was used to maximize the sum of the variance of the factor coefficients. The loadings of measured heavy metal concentrations in the

Table 3. Evaluation performance of ordinary kriged map of heavy metals through cross-validation

Heavy metals	Mean absolute error (MAE)	Mean square error (MSE)	Goodness of prediction (*G*)
Fe	25.59	329276	40
Mn	0.835	33729	46
Zn	-0.709	5109	28

Table 2. Semivariogram model and parameters of heavy metals

Heavy metals	Fitted model	Nugget (C_0)	Sill ($C+C_0$)	Range (A) (m)	Nugget/Sill
Fe	Spherical	0.258	0.592	1784	0.436
Mn	Exponential	0.403	0.697	1083	0.578
Zn	Exponential	0.315	0.752	994	0.419

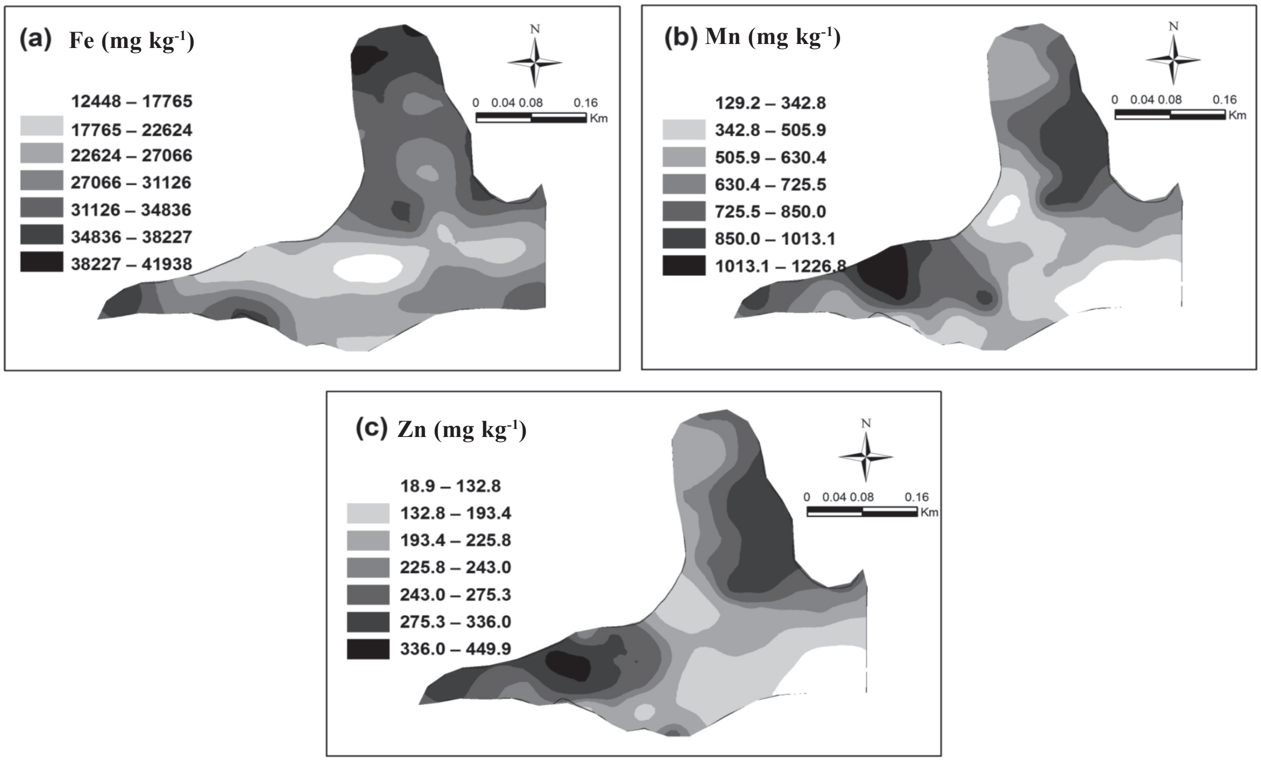

Fig. 2. Spatial distribution maps of (a) iron, (b) manganese and (c) zinc

Table 4. Matrix of the three principal components (PC) accounting for most of the total variance

Heavy metals	PC1	PC2	PC3	Communities
Fe	0.998	-0.055	0.007	1.00
Mn	0.016	0.961	0.278	0.92
Zn	0.040	0.960	-0.277	0.92
Percentage of variance	61.56	33.10	5.14	
Cumulative percent	61.56	94.66	99.80	

Table 5. Correlation-coefficients between heavy metals and soil properties and their level of significance (n = 83)

Soil properties	pH	Organic carbon	Fe	Mn	Zn
pH	1.000				
Organic carbon	-0.491**	1.000			
Fe	-0.100	0.014	1.000		
Mn	0.331**	-0.404**	-0.034	1.000	
Zn	0.304**	-0.339**	-0.014	0.846**	1.000

**Significant at P=0.01; *Significant at P=0.05

coordinate system of three principal components (PC) were obtained by analyzing the correlation matrix.

In detail, principal component 1 (PC1) has the high positive loadings of Fe (+0.998) and accounts for 61.5% of variance (Table 4) and is the most important component. The PC1 could be better explained as anthropogenic source, specifically derived from coal mine effluents. Geochemical weathering of sulphide minerals (Eqs. 6-9) derived from mine drainage leads to accumulation of Fe in the soil (Bhuiyan *et al.* 2010). Meanwhile, there were non-significant correlations between Fe with Mn and Zn in the soils of the study area (Table 5), which implied that Fe in soils might have originated from coal mine effluents. Considering the above reason, the components loading of PC1 might have been derived from coal-mine drainage sources, and PC1 might be defined as a coal mine drainage component.

The PC2, which has high positive loading of Mn (+0.961) and Zn (+0.960), accounts for 33.1% of variance. The PC2 could be considered as a measure of leaching of crustal materials because an important fraction of all the metals is lithogenic (Bhuiyan *et al.* 2010). The sulphide minerals (*e.g.* siderite and sphalerite) might be oxidized in an open environment and released Mn and Zn to soil.

Conclusions

Geostatistics and statistics have been employed for assessment and mapping of soil pollution in the waste disposal site and surrounding cultivated areas around the Ledo coal mine in the Tinsukia district of north-eastern India. A good variogram structure of heavy metals was observed, showing that there are clear spatial patterns of heavy metals on the distribution map and also that the current sampling density is sufficient to indicate such spatial patterns. The kriging interpolated map showed that high concentration of heavy metals was located in the low-lying rice field and near coal mining site. Principal component analysis and correlation matrix used in this study provide important tools for the source identification. However, further information is needed for more details about possible and real sources.

References

Adriano, D.C. (2001) *Trace elements in terrestrial environments biogeochemistry, bioavailability and risks of metals.* Springer, New York.

Banwart, S.A. and Malmstrom, M.E. (2001) Hydrochemical modeling for preliminary assessment of mine water pollution. *Journal of Geochemical Exploration* **74**, 73-97.

Bhuiyan, M.A.H., Parvez, L., Islam, M.A., Dampare, S.B. and Suzuki, S. (2010) Heavy metal pollution of coal mine-affected agricultural soils in the northern part of Bangladesh. *Journal of Hazardous Materials* **173**, 384-392.

Davis, B.M. (1987) Uses and abuses of cross-validation in geostatistics. *Mathematical Geology* **19**, 241-248.

De Marsily, M. (1986) *Quantitative hydrogeology; groundwater hydrology for engineers.* Academic Press.

Deutsch, C.V. and Journal, A.G. (1992) *Geostatistical software library and user's guide.* Oxford University Press, New York.

Franco-Uría, A., López-Mateo, C., Roca, E. and Fernández-Marcos, M.L. (2009) Source identification of heavy metals in pastureland by multivariate analysis in NW Spain. *Journal of Hazardous Materials* **165**, 1008-1015.

Franzen, D.W. and Peck, T.R. (1993) Soil sampling for variable rate fertilization. In *Proceedings of Illinois Fertilizer Conference, Jan 25–27, Urbana-Champaign* (R.G. Hoeft, Ed.), University of Illinois, pp. 81-91.

Goovaerts, P. (1999) Geostatistics in soil science: State-of-the-art and perspectives. *Geoderma* **89**, 1-45.

Journel, A.G. and Huijbregts, C.J. (1978) *Mining geostatistics.* Academic, London.

Lopez-Granados, F., Jurado-Exposito, M., Atenciano, S., Gracia-Ferrer, A., De La Orden, M.S. and Gracia-Toreres, L. (2002) Spatial variability of agricultural soil parameters in Southern Spain. *Plant and Soil* **246**, 97-105.

Mabit, L. and Bernard, C. (2007) Assessment of spatial distribution of fallout radionuclides through geostatistics concept. *Journal of Environmental Radioactivity* **97**, 206-219.

MacFarlane, G.R. and Burchett, M.D. (2002) Cellular distribution of Cu, Pb, and Zn in the grey mangrove *Avicennia marina* (Forsk.) Vierh. *Aquatic Botany* **68**, 45-59.

Madejón, P., Murillo, J.M., Maranon, T., Cabrera, F.R. and Lopez, R. (2002) Bioaccumulation of As, Cd, Cu, Fe and Pb in wild grasses affected by the Aznal collar mine spill (SW Spain). *Science of the Total Environment* **290**, 105-120.

Mueller, T.G. and Pierce, F.J. (2003) Soil carbon maps: enhancing spatial estimates with simple terrain attributes at multiple scales. *Soil Science Society of America Journal* **67**, 258-267.

Nesa, N. and Azad, P. (2008) Studies on trace metal levels in soil and water of Tipong, Tirap and Kikak collieries of Makum coal field, Tinsukia, Assam. *Pollution Research* **27**, 237-239.

Reza, S.K., Sarkar, D., Baruah, U. and Das, T.H. (2010) Evaluation and comparison of ordinary kriging and inverse distance weighting methods for prediction of spatial variability of some chemical parameters of Dhalai district, Tripura. *Agropedology* **20**, 38-48.

Reza, S.K., Baruah, U. and Sarkar, D. (2012) Spatial variability of soil properties in Brahmaputra plains of north-eastern India: A geostatistical approach. *Journal of the Indian Society of Soil Science* **60**, 108-115.

Reza, S.K., Baruah, U., Singh, S.K. and Das, T.H. (2015) Geostatistical and multivariate analysis of soil heavy metal contamination near coal mining area, northeastern India. *Environmental Earth Science.* **73**, 5425-5433.

Reza, S.K., Baruah, U. and Sarkar, D. (2013) Hazard assessment of heavy metal contamination by the paper industry, north-eastern India. *International Journal of Environmental Studies* **70**, 23-32.

Reza, S.K., Baruah, U. and Singh, S.K. (2014) Soil risk assessment of heavy metal contamination near oil refinery area, north-eastern India. *International Journal of Agriculture, Environment and Biotechnology* **7**, 787-795.

Reza, S.K., Baruah, U., Sarkar, D. and Singh, S.K. (2016a) Spatial variability of soil properties using geostatistical method: a case study of lower Brahmaputra plains, India. *Arabian Journal of Geosciences* **9**, 446.

Reza, S.K., Baruah, U., Singh, S.K. and Srinivasan, R. (2016b) Spatial heterogeneity of soil metal cations in the plains of humid subtropical northeastern India. *Agricultural Research* **5**, 346-352.

Reza, S.K., Baruah, U. and Singh, S.K. (2016c) Spatial distribution of Fe and Mn in paper mill effluent affected agricultural soils in Morigaon, Assam. *Agropedology* **26**, 87-93.

Reza, S.K., Nayak, D.C., Chattopadhyay, T., Mukhopadhyay, S., Singh, S.K. and Srinivasan, R. (2016d) Spatial distribution of soil physical properties of alluvial soils: a geostatistical approach. *Archives of Agronomy and Soil Science* **62**, 972-981.

Reza, S.K., Nayak, D.C., Mukhopadhyay, S., Chattopadhyay, T. and Singh, S.K. (2017) Characterizing spatial variability of soil properties in alluvial soils of India using geostatistics and geographical information system. *Archives of Agronomy and Soil Science* **63**, 1489-1498.

Robertson, G.P., Klingensmith, K.M., Klug, M.J., Paul, E.A., Crum, J.C. and Ellis, B.G. (1997) Soil resource, microbial activity, and primary production across an agricultural ecosystem. *Ecological Applications* **7**, 158-170.

Rose, A.W. and Cravotta, C.A. (1998) Geochemistry of coal mine drainage. In *Coal mine drainage prediction and pollution prevention in Pennsylvania* (K.B.C. Brady, M.W. Smith and J.H. Schueck Eds.), Harrisburg: Pennsylvania Department of Environmental Protection.

Sakurovs, R., French, D. and Grigore, M. (2007) Quantification of mineral matter in commercial cokes and their parent coals. *International Journal of Coal Geology* **72**, 81-88.

Schloeder, C.A., Zimmermen, N.E. and Jacobs, M.J. (2001) Comparison of methods for interpolating soil properties using limited data. *Soil Science Society of America Journal* **65**, 470-479.

Silva, L.F.O., Wollenschlager, M. and Oliveira, M.L.S. (2011) A preliminary study of coal mining drainage and environmental health in the Santa Catarina region, Brazil. *Environmental Geochemistry and Health* **33**, 55-65.

Simmons, J.A., Lawrence, E.R. and Jones, T.G. (2005) Treated and untreated acid mine drainage effects on stream periphyton biomass, leaf composition, and macro invertebrate diversity. *Journal of Freshwater Ecology* **20**, 413-424.

Voltz, M. and Webster, R. (1990) A comparison of kriging, cubic splines and classification for redicting soil properties from sample information. *Journal of Soil Science* **41**, 473-490.

Walkley, A. and Black, I.A. (1934) An examination of the digtjareff method for determining soil organic matter, and a proposed modification of the chromic acid titration method. *Soil Science* **37**, 29-38.

Warrick, A.W. (1998) Spatial variability. In *Environmental Soil Physics* (D. Hillel, Ed.), Academic Press, New York, pp. 655-675.

Webster, R. and Oliver, M.A. (2001) *Geostatistics for Environmental Scientists.* Brisbane: Wiley, pp. 225-226.

Wong, M.H. (2003) Ecological restoration of mine degraded soils, with emphasis on metal contaminated soils. *Chemosphere* **50**, 775-780.

Yao, L.X., Zhou, X.C., Cai, Y.F. and Chen, W.Z. (2004) Spatial variability of soil properties at different sampling intensities and accuracy of their estimation. *Soils* **36**, 538-542.

Zhu, X.H., Yang, X.C. and Cai, Y.L. (2005) Fractal and fractal dimension of spatial distribution of China soil system. *Acta Pedologica Sinica* **42**, 881-888.

Revised received 16 August 2017; Accepted 12 March 2018